



# CHORUS

This is the accepted manuscript made available via CHORUS. The article has been published as:

## Simple, empirical approach to predict neutron capture cross sections from nuclear masses

A. Couture, R. F. Casten, and R. B. Cakirli

Phys. Rev. C **96**, 061601 — Published 20 December 2017

DOI: [10.1103/PhysRevC.96.061601](https://doi.org/10.1103/PhysRevC.96.061601)

# A simple, empirical approach to predict neutron capture cross sections from nuclear masses

A. Couture\*

*Los Alamos National Laboratory, Los Alamos, New Mexico, 87545, USA*

R. F. Casten

*Wright Lab, Yale University, New Haven, Connecticut 06520, USA and  
Michigan State University-Facility for Rare Isotope Beams (MSU-FRIB), East Lansing, Michigan 48823, USA*

R. B. Cakirli

*Department of Physics, University of Istanbul, Istanbul, Turkey*

(Dated: December 5, 2017)

**Background:** Neutron capture cross sections are essential to understanding the astrophysical  $s$  and  $r$  processes, the modeling of nuclear reactor design and performance, and for a wide variety of nuclear forensics applications. Often, cross sections are needed for nuclei where experimental measurements are difficult. Enormous effort, over many decades, has gone into attempting to develop sophisticated statistical reaction models to predict these cross sections. Such work has met with some success but is often unable to reproduce measured cross sections to better than 40%, and has limited predictive power, with predictions from different models rapidly differing by an order of magnitude a few nucleons from the last measurement.

**Purpose:** To develop a new approach to predicting neutron capture cross sections over broad ranges of nuclei that accounts for their values where known and which has reliable predictive power with small uncertainties for many nuclei where they are unknown.

**Methods:** Experimental cross sections neutron capture cross sections were compared to empirical mass observables in regions of similar structure.

**Results:** We present an extremely simple method, based solely on empirical mass observables, that correlates neutron capture cross sections in the critical energy range from a few keV to a couple hundred keV. We show that regional cross sections are compactly correlated in medium and heavy mass nuclei with the two-neutron separation energy. These correlations are easily amenable to predict unknown cross sections, often converting the usual extrapolations to more reliable interpolations. It almost always reproduces existing data to within 25% and estimated uncertainties are below about 40% up to 10 nucleons beyond known data.

**Conclusions:** Neutron capture cross sections display a surprisingly strong connection to the two-neutron separation energy, a nuclear structure property. The simple empirical correlations uncovered provide model independent predictions of neutron capture cross sections, extending far from stability, including for nuclei of the highest sensitivity to  $r$ -process nucleosynthesis.

PACS numbers: 21.10.Ft, 21.10.-k, 21.10.Dr

Knowledge of neutron capture cross sections is critical to understanding the synthesis of the elements in stellar sites, which has been identified as one of the most important quests in science, as well as in many areas of practical application, ranging from reactor design to nuclear forensics. Unfortunately, these cross sections can vary by orders of magnitude, even for nearby isotopes, and existing theoretical approaches, despite decades of work, often differ by large amounts for keystone nuclei of astrophysical importance [1–4]. Indeed, we are presently limited in our ability to use astrophysical abundance signatures to understand neutron-star mergers, core-collapse supernovae, and more exotic explosions, due to poor knowledge of critical capture cross sections at temperatures from  $kT=1-500$  keV [4–6].

The purpose of this manuscript is to present an ex-

remely simple, physics-based approach to correlating and predicting neutron capture cross sections over much of the nuclear chart exploiting a newly discovered connection with nuclear masses.

Elements beyond iron are made predominantly through neutron capture processes since fusion reactions of heavy elements are endothermic. The slow ( $s$ ) and rapid ( $r$ ) neutron capture processes are postulated to account for the observed abundance distributions of heavy elements [7, 8]. The  $s$  process takes place on a timescale slow relative to beta decay, relatively near stability, and accounts for the synthesis of approximately half of the observed isotopes heavier than iron. The  $r$  process, thought to produce isotopes from Fe to the actinides [9], takes place over a timescale of seconds in conditions of extreme neutron density in nuclei far from stability where direct measurements are not possible. Substantial uncertainties remain in the astrophysical site of the  $r$  process, with neutron-star mergers and core-collapse supernovae being prime candidates. In both scenarios, our understanding

---

\*Corresponding Author: [acouture@lanl.gov](mailto:acouture@lanl.gov)

of these sources of nucleosynthesis is limited due to lack of knowledge of critical capture cross sections in the energy range from a few to several hundred keV. Recent systematic assessments have identified the highest impact cross sections [5, 10]. Many of these are on unstable isotopes, which are, optimistically, difficult to measure.

In nuclear reactors, neutron capture is a poison, absorbing neutrons that could otherwise induce fission and release energy. Further, as fission products build up, neutron capture can transmute those materials, affecting the operational safety and waste stream of the reactor [11]. In nuclear forensics, neutron capture is an essential diagnostic and, again, capture cross sections on key isotopes are unknown yet critical for successful applications.

Since 1952, sophisticated theoretical methods, typically using Hauser-Feshbach statistical approaches, and incorporating numerous ingredients, ranging from spin cutoffs, to pairing effects, to level density estimates, and incorporating degrees of freedom such as  $M1$  or  $E1$  collective modes, and giant resonance behavior, have been used to estimate such cross sections [1, 3, 12, 13]. Nevertheless, predictive accuracy near stability is often no better than factors of 2-5, and seldom more reliable than 30-50% [1, 3]. Predictions of different approaches often differ by large factors for unstable nuclei, making estimates challenging. The situation can be seen in Figure 1. If we compare experimental results to the statistical model codes TALYS and NON-SMOKER in the rare earth region, we characteristically see deviations of 20-50% or more throughout for nuclei with known cross sections. Further, we show the ratio of TALYS to NON-SMOKER predictions for the Hf isotopes in the lower part of Fig. 1. These Hf isotopes are well-behaved from the perspective of Hauser-Feshbach calculations. Yet, the models disagree by a factor of 2 for some stable isotopes, and quickly deviate by factors  $> 5$  for isotopes just a few neutrons off stability.

Great effort has gone into measuring key needed cross sections, but the experiments are difficult and costly [2, 14, 16]. The preferred technique uses a neutron beam impinging on targets of the isotope of interest, limiting measurements to those on isotopes with half-lives of at least tens of days [17]. Both theoretical and experimental efforts continue but there is a critical need for a more reliable approach, less susceptible to unknown factors, including level densities, gamma strength functions, and collective modes.

In this manuscript, we propose a simple, empirical approach that allows one to tightly correlate neutron capture cross sections and nuclear masses. The correlations are quite compact and robust (with certain caveats, see below), and allow for accurate estimates of unknown cross sections, sometimes even by interpolation. Moreover, estimates of new cross sections are readily obtainable when new masses are measured further from stability. These results may partially obviate the need for relying solely on theoretical modeling, especially in unstable nuclei or, alternately, perhaps help in improving the parametrization in those models, and may reduce the

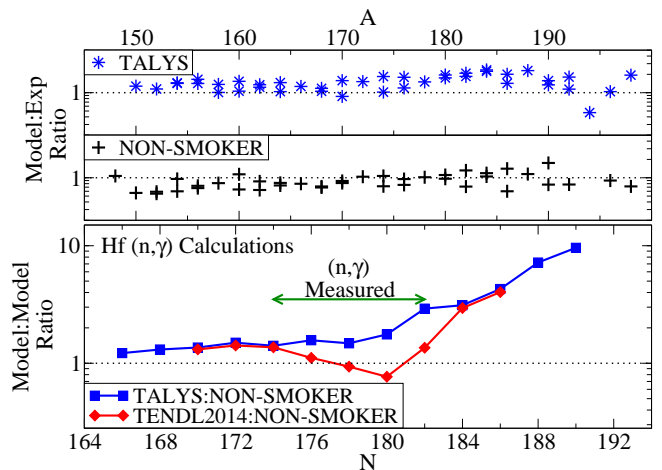


FIG. 1: (Color online) In the upper panel the ratio of default TALYS and NON-SMOKER model predictions to experimental cross sections from Ref. [1, 3, 14] are shown. A ratio of 1.0 implies the model reproduces the measurement. The lower panel shows the ratios of different models. TENDL2014 [15] is constrained by measurements, and largely agrees with experiment where measurements exist, but quickly approaches default TALYS calculations off stability.

need for certain especially difficult experiments.

The challenge is illustrated in Fig. 2a), adapted from Ref. [2], which shows measured Maxwellian-averaged neutron capture cross sections (MACS) at  $kT = 30$  keV. Astrophysically relevant, the MACS typically integrates over many resonances [18]. Clearly there is a systematic, overall bell-shaped dependence on neutron number with sequential shifts with  $Z$ , but using these results for predictions is risky.

The general behavior in Fig. 2a) is easy to understand. There are three main ingredients: the number of valence nucleon configurations, the fraction of these at any given excitation energy, and the excitation energy at which the capture state lies.

As nucleons are added from a closed shell, the number of possible valence shell configurations allowed by the Pauli Principle grows combinatorially. For example, for two valence nucleons in a  $g_{7/2}$  orbit there is only one  $2^+$  state. For the 22 valence protons and neutrons in  $^{154}\text{Sm}$ , there are approximately  $3 \times 10^{14}$ . Therefore the density of states grows with valence nucleon number and is reflected in the growth in the cross sections just above  $N = 82$  in Fig. 2a).

Continuing into the shell, there is a competition between the growth in the number of configurations at the capture state energy and the decrease in that energy as successively added neutrons are less bound, leading, after  $N \approx 90$ , to a reduced density of states in the Maxwellian energy window. Qualitatively, this accounts for the sharp drop as a function of  $N$  seen in Fig. 2a), beyond  $N \approx 94$ .

At the same time, the capture state energy increases with  $Z$  as the neutrons are more bound by the greater number of protons. This accounts for the increase in cross

sections with  $Z$  in Fig. 2a) for a given neutron number.

Despite these qualitative ideas, exploiting them to make specific predictions is a challenging task and elusive goal. No general method has yet been shown to correlate the cross sections well enough to satisfy the desired accuracy for predicting stellar nucleosynthesis or for practical applications.

Inspired by Fig. 2a), we have discovered a new correlation. We illustrate our principle result in Fig. 2b), which shows all the  $kT = 30$  keV experimentally measured Maxwellian averaged cross sections for deformed and transitional even-even nuclei from  $^{148}\text{Nd}$  through  $^{184}\text{W}$  in the well-studied rare earth region  $Z = 50 - 82$ ,  $N = 82 - 126$ , plotted simply against the two-neutron separation energy,  $S_{2n}(N+2)$ . The figure reveals a very tight correlation of cross sections with  $S_{2n}(N+2)$  which is the main result of this work. Despite its simplicity, this correlation has not been recognized before.

Note that we evaluate the two-neutron separation energy at  $N+2$  rather than  $N$  to reflect the average separation energy of the neutrons actually deposited. One might have expected the cross sections to correlate well with  $S_{1n}$ , and they do, but not as well as for  $S_{2n}$ , presumably because of the role of varying single particle, pairing, and rotational effects that come into  $S_{1n}$ .

To exploit this correlation to predict unknown cross sections (see below), Fig. 2 b) also includes a least squares fit to the data (including their uncertainties) using a simple scaled power law in  $S_{2n}(N+2)$ , which is given in the legend. This function is solely intended to fit the trends and, intentionally, is not based on, or biased by, any particular theory. Correlations in the fit parameters were considered explicitly in order to determine the fit uncertainty based on the covariance matrix of the fit. Shown in the lower panel of Fig. 2 b) are the relative deviations of the fit from the experimental measurements. Nearly all of the values lie within a factor of 1.25 of the experimental cross-section. As a metric of the goodness-of-fit, we report the geometric root-mean-square deviation,  $f_{rms}$  given by

$$f_{rms} = \exp \left\{ \left[ \frac{1}{N} \sum_i \left( \ln \left( \frac{\sigma_{emp}}{\sigma_{exp}} \right) \right)^2 \right]^{\frac{1}{2}} \right\} \quad (1)$$

For the even-even rare-earth nuclei illustrated in Fig. 2b),  $f_{rms}=1.24$ , where perfect reproduction of the data would give a value of 1. We note that this metric does not account for the experimental uncertainties which were included in the fit and the reported fit uncertainty. Because of the nature of the data, the geometric RMS more accurately represents the fit quality than a more traditional arithmetic RMS.

Thus far we have discussed nuclei in the transitional and deformed rare earth region. We have found similar correlations in other regions, though with fewer measured cross sections. Due to differences in the number of configurations, and to structural differences in different sets

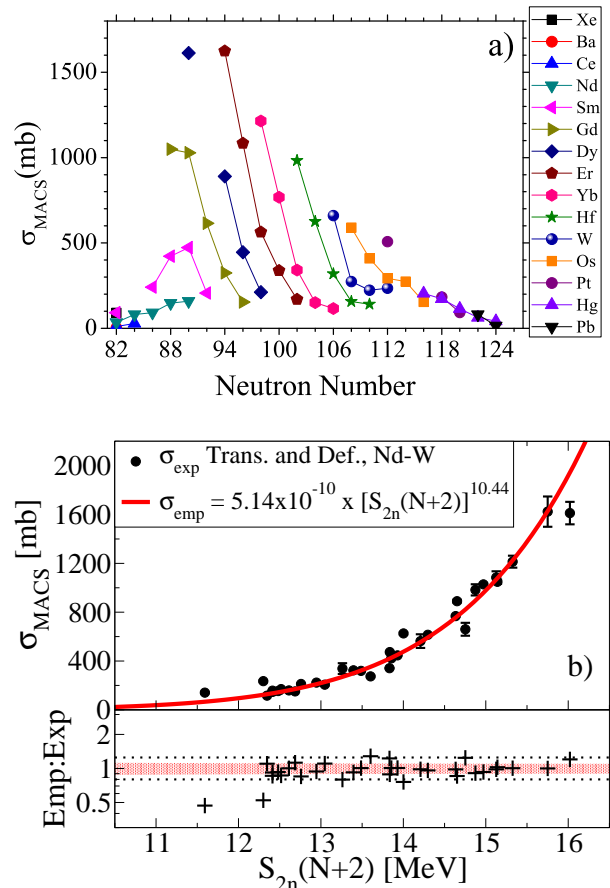


FIG. 2: (Color online) a) Maxwellian averaged experimental cross sections at 30 keV for the rare earth region plotted against neutron number [14]. Shown in b) are the experimental neutron capture cross sections at  $kT = 30$  keV plotted versus  $S_{2n}(N+2)$ , as discussed in the text [14, 19]. The fit function is given in the legend and the uncertainty (pink band) is  $\Delta\sigma_{MACS} = [S_{2n}(N+2)]^{9.44} (4.33 \times 10^{-21} [S_{2n}(N+2)]^2 - 6.89 \times 10^{-20} S_{2n}(N+2) + 6.89 \times 10^{-19})^{1/2}$ . In the plot of the ratio of the empirical fit to the data, the horizontal dotted lines indicate a 25% deviation. The ratio is shown on a log scale so that the visual scale of a factor of two difference is maintained.

of nuclei, the curves turn out to be region-dependent and must be developed from known data for each region.

In the same shell as Fig. 2b), there are a number of spherical nuclei in Ce, Nd and Hg isotopes where  $R_{4/2} < 2.6$ . Although their systematics looks very different from the deformed nuclei in Fig. 2a), their behavior illustrated in Fig. 3a) has exactly the same overall trend as in Fig. 2b). The Os and Pt nuclei are well-known to be highly axially symmetric,  $\gamma$ -soft, and even undergo a prolate-oblate shape transition near  $N \approx 116$ . The neutron cross sections again show a similar correlation with  $S_{2n}(N+2)$  as shown in Fig. 3b). In Fig. 3c) we show lighter nuclei, in the  $Z = 50 - 82$ ,  $N = 50 - 82$  region. Once again, the correlation is very tight. In the actinides,

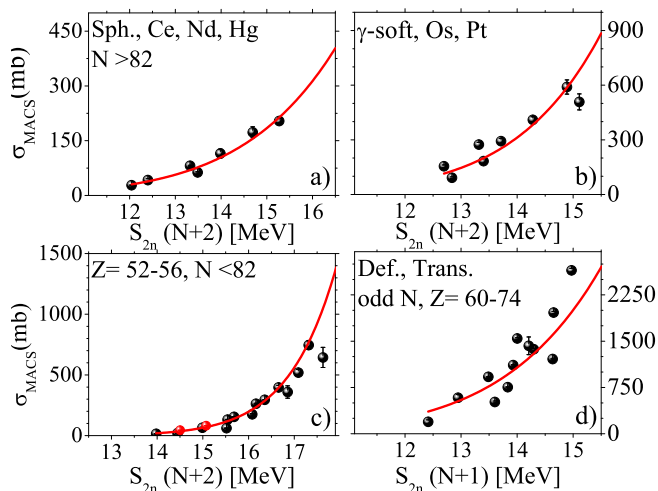


FIG. 3: (Color online) Similar to Fig. 2b) for different sets of nuclei. In each panel the nuclei shown are summarized at the top left. The fit functions are as follows: a)  $\sigma_{emp} = 3.98 \times 10^{-8} \times S_{2n}(N+2)^{8.22}$ , b)  $\sigma_{emp} = 5.8 \times 10^{-10} \times S_{2n}(N+2)^{10.23}$ , c)  $\sigma_{emp} = 3.45 \times 10^{-19} \times S_{2n}(N+2)^{17.24}$ , d)  $\sigma_{emp} = 4.27 \times 10^{-8} \times S_{2n}(N+1)^{9.07}$ . In c), the two red points correspond to the nuclei  $^{126,128}\text{Te}$  for which  $D_0 > 400$  eV.

few cross sections are known and their uncertainties are larger, hence we do not illustrate these. However, the existing actinide data are consistent with these trends.

Finally, in even-odd deformed nuclei in the rare earth region of deformed nuclei (see Fig. 3d), pairing correlations are reduced giving a higher density of states at a given excitation than in even-even nuclei and shifting the correlation to a lower  $S_{2n}$ . Note that for even-odd nuclei we use  $S_{2n}$  at  $N+1$  to again reflect the actual separation energy of the deposited neutrons.

As encouraging as these results are, the method does break down in some cases in lighter nuclei as illustrated for  $Z = 42 - 48$ ,  $N = 50 - 82$ , in Fig. 4 where protons fill a single  $j$ -shell,  $1g_{9/2}$ , and neutrons primarily occupy a small space consisting of  $2d_{5/2}$ ,  $1g_{7/2}$  orbits. This configuration space might be too small to generate sufficient level density in the capture state region for adequate averaging of the Maxwellian distributed neutron energies. Indeed, while known  $s$ -wave level spacings,  $D_0$ , are mostly  $< 30$  eV in deformed rare earth nuclei they often exceed 1000 eV in the Zr-Sn region. Such low level densities may also be the reason that no useful correlations are found for singly magic nuclei (e.g., Sn, Pb, or the  $N = 82$  isotones).

We have discussed the 30 keV cross section data. However, cross sections are needed at other energies as well for both the  $s$  and  $r$  processes. The same correlations are observed, and can be used for predictions of unknown cross sections. To illustrate this we show the results for the same nuclei as in Fig. 2b) for energies of 5 and 100 keV in Fig. 5.

We have mentioned that these correlations can be used to provide improved predictions for capture cross sections

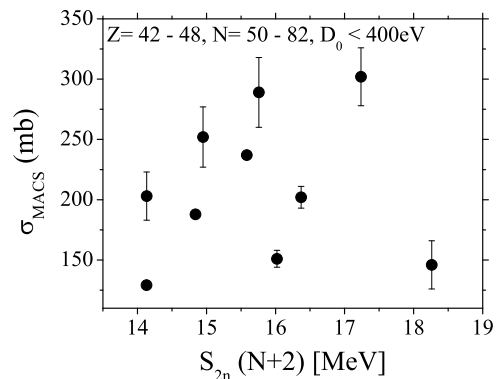


FIG. 4: (Color online) Similar to Fig. 2b), for the region  $Z = 42 - 48$ ,  $N = 50 - 82$ , for nuclei for which  $D_0 < 400$  eV. No fit is shown because no reasonable correlation emerges.

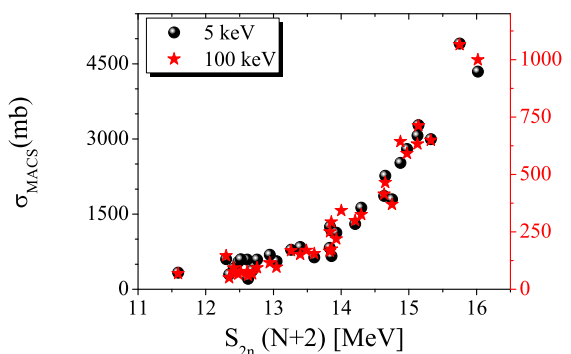


FIG. 5: (Color online) Cross sections for the same nuclei as in Fig. 2b), at average neutron energies of: a) 5 keV and b) 100 keV.

where they have not or cannot be measured and where theories tend to diverge (See Fig. 1). Table I includes predictions for a selected set of nuclei that have been identified as of highest sensitivity for understanding astrophysics environments [6, 10] in the rare earth region. Isotopes of interest to nuclear forensics are also predicted. Many others can be predicted, as needed. The predictions were made using the fit function in Fig. 2b). They are facilitated because  $S_{2n}$  values have become more easily and accurately measurable in the past two decades with storage-ring and Penning-trap mass spectrometry techniques, even for many unstable nuclei, and hence are known for many more nuclei than neutron capture cross sections [20]. Examples in Table I are  $^{158}\text{Sm}$  and  $^{154,156}\text{Dy}$ . In other cases, the  $S_{2n}$  values had to be estimated. However, it is well known that, except at closed shells and in regions of rapid shape change,  $S_{2n}$  values behave very nearly linearly with neutron number, and with slopes that are highly correlated as a function of  $Z$  [19]. Thus the uncertainties in extrapolated  $S_{2n}$  values are small (See Table I) and the consequent uncertainties in the predictions from this source are also generally small.

TABLE I: Predictions of 30 keV MACS for selected nuclei chosen because of the sensitivity of the  $r$  process to their cross sections as summarized in Ref. [6, 10], along with several neutron-deficient nuclei to give an indication of how the predictions and their uncertainties vary. Shown in parentheses in the second and third columns are the uncertainties on the last digits. The fourth and fifth columns give the independent individual uncertainties, in the same units, from the fit function and in the  $S_{2n}$  values.

Nucleus	$S_{2n}(N+2)$ [MeV]	$\sigma_{MACS}$ [mb]	$\Delta\sigma_{MACS}$ (fit)	$\Delta\sigma_{MACS}$ ( $\Delta S_{2n}$ )
$^{156}\text{Nd}$	9.881 (40)	12.6 (17)	(16)	(5)
$^{158}\text{Nd}$	8.970 (80)	4.57 (78)	(64)	(44)
$^{160}\text{Nd}$	8.060 (120)	1.50 (34)	(23)	(25)
$^{162}\text{Nd}$	7.149 (160)	0.43 (13)	(8)	(11)
$^{158}\text{Sm}$	11.127 (8)	43.4 (51)	(51)	(3)
$^{160}\text{Sm}$	10.167 (40)	16.9 (23)	(21)	(7)
$^{162}\text{Sm}$	9.206 (80)	6.00 (100)	(82)	(57)
$^{164}\text{Sm}$	8.246 (120)	1.90 (42)	(29)	(31)
$^{166}\text{Sm}$	7.286 (160)	0.52 (16)	(9)	(13)
$^{168}\text{Sm}$	6.325 (200)	0.12 (5)	(2)	(5)
$^{168}\text{Gd}$	8.849 (160)	3.97 (99)	(56)	(82)
$^{154}\text{Dy}$	16.278 (9)	2310 (233)	(233)	(10)
$^{156}\text{Dy}$	16.021 (7)	1950 (198)	(198)	(10)
$^{174}\text{Dy}$	8.030 (160)	1.44 (40)	(22)	(33)
$^{174}\text{W}$	16.557 (40)	2750 (286)	(277)	(70)
$^{176}\text{W}$	15.908 (40)	1810 (190)	(184)	(50)
$^{178}\text{W}$	15.372 (32)	1270 (133)	(130)	(30)

Enhancing further the usefulness of such predictions is the fact that  $S_{2n}$  values for nuclei with unknown cross sections are often within the range of known cases *e.g.*, between about 11.4 and 16.4 MeV in Fig. 2b). Therefore, those predictions often only require interpolation and their expected accuracy is simply given by the scatter of points around the best fit curve in Fig. 2b). Note, finally, that, as new  $S_{2n}$  values are measured, these predictions can be refined.

In conclusion, in heavy nuclei we have discovered a previously unrecognized connection between a nuclear structure property,  $S_{2n}$ , and a nuclear reaction property, the neutron capture cross section. The neutron capture reaction plays a critical role in determining the elements

produced in the universe as well as in interpreting and designing man-made nuclear energy environments. All of these scenarios require reliable reaction rate predictions for short-lived isotopes that are not straightforward to study. Our simple parametrization of the cross sections achieves comparable or better precision in reproducing known cross sections as much more detailed and complex theoretical treatments. Further, it has the advantage that it depends on a nuclear observable ( $S_{2n}$ ) that is relatively straight-forward to measure experimentally, even for isotopes far from stability, and easier and more reliable to extrapolate compared to neutron capture cross sections. Hence, as new mass measurements become available, the reliability of  $(n, \gamma)$  predictions from our treatment will also improve. Our method differs from traditional theoretical approaches in several ways. First, it is empirical. Second, it is based explicitly on a single variable. This correlation highlights a sensitivity of neutron capture to the excitation energy of the capture state, while the regional or structural differences in the correlation may reflect other facets such as the number of valence configurations and consequently the level density at any given capture state energy. As such, as has been shown, the correlations are region dependent and need to be calibrated to and tested against known cross sections to determine the correlation in each given region. In addition to explicit predictions, this may provide useful insights for future modeling via Hauser-Feshbach or other techniques.

### Acknowledgments

We are grateful to Toshihiko Kawano, Matthew Mumpower, Klaus Blaum, and Keegan Kelly for useful discussions. This material is based upon work supported by the U.S. Department of Energy, National Nuclear Security Administration, under contract number DE-AC52-06NA25396. R.F.C. acknowledges support from MSU-FRIB and LANL. R.B.C. acknowledges support from the Max-Planck Partner group, TUBA-GEBIP, and Istanbul University Scientific Research Project No. 54135.

- 
- [1] T. Rauscher and F.-K. Theilemann, *Atomic Data and Nuclear Data Tables* **79**, 47 (2001).
- [2] Z. Y. Bao, H. Beer, F. Käppeler, F. Voss, K. Wisshak, and T. Rauscher, *At. Data and Nucl. Data Tabl.* **76**, 70 (2000).
- [3] A. Koning, S. Hilaire, and M. Duijvestijn, *Talys 1.8* (2006), [www.talys.eu](http://www.talys.eu), URL [www.talys.eu](http://www.talys.eu).
- [4] K. Farouqi, K. Kratz, B. Pfeiffer, T. Rauscher, F. Thielemann, and J. W. Truran, *Astrophys. J.* **712**, 1359 (2010).
- [5] M. Pignatari, R. Gallino, M. Heil, M. Wiescher, F. Käppeler, F. Herwig, and S. Bisterzo, *Ap. J.* **710**, 1557 (2010).
- [6] M. R. Mumpower, R. Surman, G. C. McLaughlin, and A. Arahmanian, *Progress in Particle and Nuclear Physics* **86**, 86 (2016).
- [7] E. M. Burbidge, G. R. Burbidge, W. A. Fowler, and F. Hoyle, *Rev. of Mod. Phys.* **29**, 547 (1957).
- [8] A. G. W. Cameron, *Annual Review of Nuclear and Particle Science* **8**, 299 (1958).
- [9] G. Wallerstein, I. Iben, P. Parker, A. M. Boesgaard, G. M. Hale, A. E. Champagne, C. A. Barnes, F. Käppeler, V. V. Smith, R. D. Hoffman, et al., *Rev. Mod. Phys.* **69**, 995 (1997).

- [10] M. R. Mumpower, G. C. McLaughlin, and R. Surman, *Phys. Rev. C* **86**, 035803 (2012).
- [11] G. Aliberti, G. Palmiotti, M. Salvatore, T. K. Kim, T. A. Taiwo, M. Animescu, I. Kodeli, E. Sartori, J. C. Bosq, and J. Tommasi, *Annals of Nuclear Energy* **33**, 700 (2006).
- [12] W. Hauser and H. Feshbach, *Phys. Rev.* **87**, 366 (1952), URL <https://link.aps.org/doi/10.1103/PhysRev.87.366>.
- [13] B. Margolis, *Phys. Rev.* **88**, 327 (1952), URL <https://link.aps.org/doi/10.1103/PhysRev.88.327>.
- [14] I. Dillmann, R. Plag, F. Käppeler, and T. Rauscher, in *EFNUDAT Fast Neutrons - scientific workshop on neutron measurements, theory & applications*, edited by F.-J. Hambsch (2009), <http://www.kadonis.org>, URL <http://www.kadonis.org>.
- [15] A. J. Koning, D. Rochman, S. van der Marck, J. Kopecky, J. C. Sublet, S. Pomp, H. Sjostrand, R. Forrest, E. Bauge, H. Henriksson, et al., *Tendl-2014: Talys-based evaluated nuclear data library file* (2014), <ftp://ftp.nrg.eu/pub/www/talys/tendl2014/tendl2014.html>, URL <ftp://ftp.nrg.eu/pub/www/talys/tendl2014/tendl2014.html>.
- [16] M. Heil, F. Käppeler, E. Uberseder, R. Gallino, and M. Pignatari, *Phys. Rev. C* **77**, 015808 (2008), URL <http://link.aps.org/doi/10.1103/PhysRevC.77.015808>.
- [17] A. Couture and R. Reifarth, *Atomic Data and Nuclear Data Tables* **93**, 803 (2007).
- [18] H. Beer, F. Voss, and R. R. Winters, *Astrophys. J. Suppl. Ser.* **80**, 403 (1992).
- [19] M. Wang, G. Audi, F. Kondev, W. Huang, S. Naimi, and X. Xu, *Chinese Physics C* **41**, 030003 (2017), URL <http://stacks.iop.org/1674-1137/41/i=3/a=030003>.
- [20] K. Blaum, *Phys. Rep.* **425**, 1 (2006).